Experimental Investigation Of The Aerodynamics Of A Single-Stage High-Speed Low-Pressure Turbine

Antonino Federico Maria Torre

Turbomachinery and Propulsion Department, von Karman Institute for Fluid Dynamics, Belgium, antonino.torre@vki.ac.be

Supervisor: Sergio Lavagnoli

Associate Professor,Turbomachinery and Propulsion Department, von Karman Institute for Fluid Dynamics, Belgium, lavagnoli@vki.ac.be

University Supervisor: Koen Hillewaert

Dpartement darospatiale et mcanique, University of Liege, Belgium, koen.hillewaert@uliege.be

Abstract

The High-Speed Low-Pressure Turbine is a key component to enable modern Ultra High By-Pass Ratio Geared TurboFan. VKI undertakes an extensive experimental campaign to investigate in a rotating turbine rig the unsteady interaction of endwall and mainstream flows with purge and leakage flows in modern LPT. This paper introduces the preliminary design selections for the new LPT module testing.

Keywords: High-Speed Low-Pressure Turbine, Annular Rotating Rig, Purge flows, Tip leakage flows, Secondary flows, Unsteady flows

1. Introduction

According to the International Civil Aviation Organization (ICAO) forecast, a 4.2% annual growth of the revenue passenger per kilometer is expected for the next 30 years [1] . The European Commission directives for 2050 Europes vision for Aviation target a 75% reduction in CO2 emissions, 90% reduction of NOx and 65% reduction in perceived noise with respect to the levels of new 2000 aircrafts [2]. Greener and more efficient propulsive units are key factors to meet these objectives. The Ultra High By-Pass Ratio Geared TurboFan (GTF) is one of most promising innovative engine architecture that is leading the transition towards a greener air traffic. Its design incorporates a gearbox that decouples the fan and low-pressure turbine (LPT). The two comonents are now designed to operate at their optimal workspace. Kurzke [3] argues that, for by-pass ratios higher than 10, the GTF enables a substantial reduction of specific fuel consumption (SFC), weights and parts counts, while the turbine high circumferential velocity enables higher turbine efficiency levels. According to Torre et al. [4], the efficiency gains are to be attributed to reduction in profile losses because of higher pitch-to-chord ratios, and reduction of the secondary flows strength due to the lower blade turning characteristic of high-speed LPTs. On the contrary, the increase in rotational speed of the LPT yields new challenges that must be addressed at structural and an aerodynamic design levels. From a mechanical point of view, the increase in rotational speed of the LPT imposes critical aeromechanical constraints due to large centrifugal stresses, Giovannini et al. [5], and increased gas loads due to the higher pressure ratios, Malzacher et al. [6]. While conventional low pressure turbines are already subjected to low Reynolds number, its combination to Mach numbers close to the unity is the most challenging new aerodynamic feature of the new LPT module [6].

Rigorous and extensive testing is of primary importance to develop a detailed understanding of these operating conditions. Linear cascade testing is an attractive option to test in detail the aerodynamics of high aspect-ratio LPT airfoils in a controlled environment. This configuration have been widely used in 2D configuration, focusing on Reynolds number effects, blade-wake interaction and compressibility ef-

fects on the blade profile ([7] [8] [9]), and to assess the quasithree-dimensional (quasi-3D) blade-to-blade flow field. A large body of literature is available on subsonic turbine cascade investigations of end-wall flows rising from the development of boundary layer ([10], [11]) and on cavity purge flows interaction with secondary end-wall and main stream flows [12]. However, linear cascades found limits to reproduce truly periodic boundary blade-to-blade flow through a finite number of airfoils, and to simulate the radial pressure gradient, which effect is significant on secondary flow formation. Annular rotating rigs provide engine-realistic testing environment, multi-row configuration and versatile adaptability for testing at on and off-design conditions ([13]). Typical three-dimensional sources of losses are investigate such as the relevant impact cavity purge flows have on the stage efficiency. Jenny et Al. ([14]) study a 1.5 stage conventional LPT with profiled endwalls contouring at three purge injection rates. The impact of purge flow injection rates show the total-to-total efficiency decrease with increasing injection rate with an efficiency deficit of 1.3% per injected percent of purge flow. Although during the last years, High-Speed LPT have been gaining visibility there is a shortage in experimental data and knowledge of typical flow regimes experienced in the new module. A systematic research approach is needed to investigate in detail the unsteady interaction between purge flows and leakage flows with the mainstream in multi-row environment, representative of modern turbine modules.

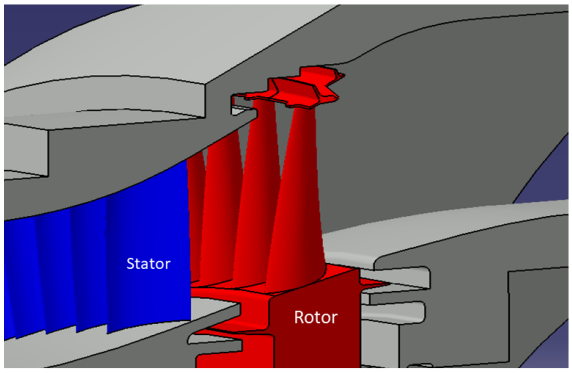

Figure 1: SPLEEN High-Speed Low-Pressure Turbine test section

2. SPLEEEN Project

The current research targets the investigation and understanding of the unsteady aerodynamics of the next-generation high-speed LPTs and is part of a large EU-funded program named SPLEEN (Secondary and Leakage Flow Effects in High-SPeed Low-PrEssurE TurbiNes) led by the von Karman Institute in collaboration with Safran Aircraft Engines (SAE). The project SPLEEN envisages the adaptation of the short-duration rotating turbine test rig of the von Karman Institute to study three-dimensional flows under engine realistic conditions. This facility will be used to conduct an extensive experimental campaign to detail the unsteady interaction between cavity purge, leakage and, secondary flows, as well the underlying loss mechanisms of high-speed LPT geometries. The cavity flow effects and the turbine unsteady 3D aerodynamics will be investigated in the Isentropic Compression Tube Annular Cascade Facility CT-3, operating at engine Mach and Reynolds numbers. The target of the measurements is to use high-resolution instrumentation to characterize the cavities aerodynamics, to quantify the stage loss and the unsteady interactions between the cavity and endwall flows. The impact of purge streams on the LPT rotor row will be measured for various purge flow rates and at off-design conditions. The output of this project will be an open-access database of high-fidelity measurements under that will contribute to develop and mature endwall models, provide boundary conditions and validation data for high-fidelity numerical simulations, and ultimately provide guidelines for the design and development of future high-speed LPTs.

3. Experimental Apparatus

3.1. Turbine Stage

The turbine module incorporates the one-to-one scale geometries of the first stage of the High Speed LP turbine (Fig. 1). Stator vanes ensure the aimed swirling flow and rotor inlet Mach number. The blade design was done to recreate the aerodynamic behavior of an intermediate stage High Speed LPT thus ensuring that the operating conditions meet the research interest. More details about the aerodynamic design of the stage are given in Table 1. The blade airfoil design features area taper form hub to tip, typically enabled to reduce the stress levels in fast spinning blades with high aspect ratios. A light interlocking shroud features the blade with two sealing teeth with a nominal tip clearance of 0.7 mm. Up and Downstream of the rotor, two hub cavities are included to perform purge flow injection, fed by discrete injecting points equally spaced over the annulus. The purge injection will allow investigating the effect of secondary air flows on

Table 1: Summary of rows geometries characteristics and flow quantities at midspan

Parameter	Value
Number of Vanes	96
Number of Blades	96
Vane outlet angle, a2 (deg.)	66.3
Blade relative inlet angle, 2 (deg.)	29.9
Blade relative angle change, (deg.)	94,8
Blade absolute exit angle, a3 (deg.)	-28.8
Vane Axial Chord $C_{ax,V}$ (mm)	32
Blade axial Chord$C_{ax,Bl}$(mm)	30
Vane aspect ratio, AR_V	3.49
Blade aspect ratio, AR_Bl	3.46
Stage Load at rotor inlet, Ψ	1.68
Flow Coefficient at rotor inlet, ϕ	0.59
Degree of reaction, DoR	45%
Specific Work (J/Kg K)	152.03

the LP blade aerodynamics. The operating conditions of the 1-stage LP test turbine can be seen in Table 2 alongside the operating conditions of the engine. As it can be seen all engine operating conditions are virtually matched with the test turbine.

3.2. Turbine Test Rig

The new module of the High-Speed Low Pressure Turbine is tested in the Von Karman Institute compression tube facility CT-3. The cross-section of the CT-3 experimental facility is represented in Fig. 2. This short duration facility can reproduce independently temperature ratios and Reynolds and Mach numbers of the actual engine conditions. The facility consists of two volumes, initially separated by a fast-acting shutter valve. The upstream compression tube contains a free piston while the downstream turbine stage is connected to the dump tank through a variable sonic throat. Prior to the experiments, the initial pressure in the tube is set and the test section (and dump tank) are evacuated to an absolute pressure of about 30 mbar. During the run-up, the rotor is accelerated by means of a small air turbine. Once the rotor nearly reaches its nominal rotational speed, air from the high-pressure reservoirs is injected at the back of the piston, which forces it to slide forward, quasi-isentropically compressing the fluid upstream of the shutter valve. When the target pressure and temperature are achieved inside the tube, the shutter valve opens. This allows the hot gas to be released into the turbine stage towards the dump tank during an actual testing time of about 400-500 ms. The operation cycle is described with further details by Sieverding and Arts [15].

Table 2: Operating Condition: Engine vs Rig

Parameter	Engine	Rig
Mass flow rate, (kg/s)	19.69	10.57
Rotational speed, rpm	7571	4466
Blade Tangential Velocity	288	170
Blade Exit Mach, M3r	0.774	0.776
Reynolds number, Re1	$1.95x10^5$	$2.10x10^5$
$U_m/\sqrt{\gamma RT_{01}}$	0.468	0.474
$\dot{m}\sqrt{RT_{01}}/D^2P_{01}\sqrt{\gamma}$	0.0701	0.0692

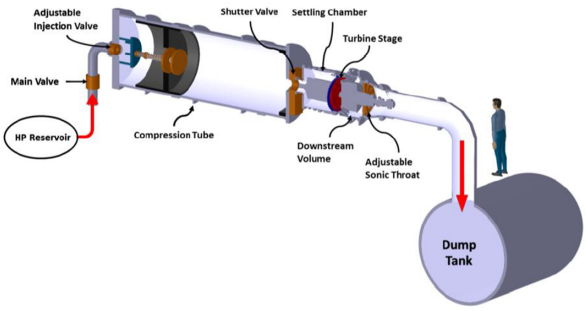

Figure 2: CT-3 compression tube facility overview

3.3. Measurement location and Instrumentation

To ensure a dense measurement matrix and high resolution data in our short duration facility, the test section will be heavily instrumented as represented in Fig. 3. A large number of time-averaged and time-resolved measurements will be taken across the turbine using a variety of stationary and traversable instrumentation. Within the gaspath, three measurement location are distinguished as stage entrance, rotor entrance and rotor outlet. Fixed measurement is envisaged at the two hub and rotor shroud cavities. In this section, every location point is discussed in detail.

3.3.1. Turbine inlet measurements Plane 1

Measurements at the inlet of the turbine are targeted to characterize total inlet flow conditions (total pressure and temperature) as well as the inlet boundary layer thickness, flow angles and turbulence intensity. These measurements will be used to obtain the status of the flow at the inlet to the stage and thus, for providing detailed inlet boundary conditions for accompanying CFD studies. The measurement plane is located approximately 2 axial chords upstream of the

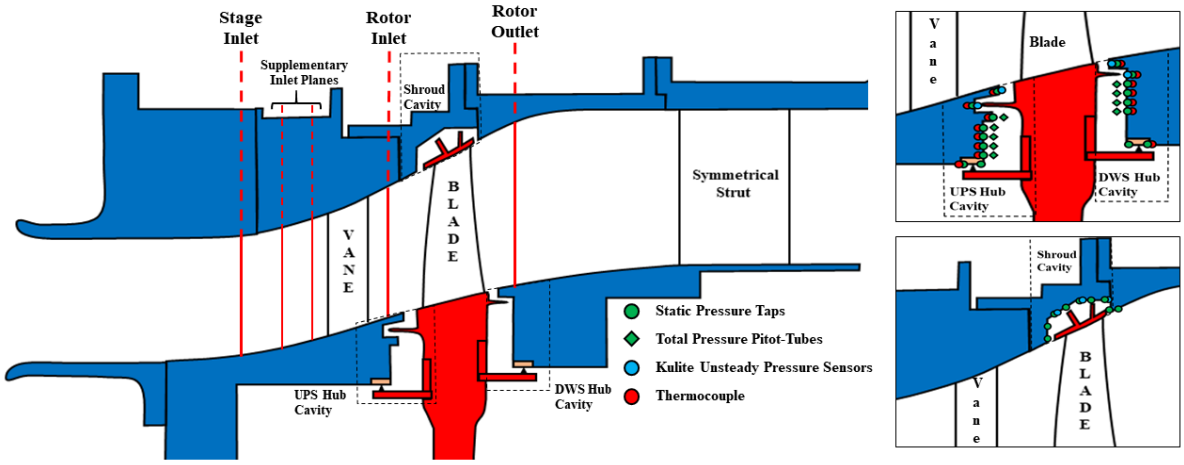

Figure 3: Stage meridional view and measurement planes (Left), Instrumentation on hub (Top-Right) and shroud cavities (Bottom-Right)

vane Leading edge. Only radial traverses are envisaged at this measurement points. The flow periodicity will be assessed by means of static pressure taps equally spaced around the annulus. Turbulence decay will be assessed by supplementary planes located further downstream between Plane 1 and Vane 1 LE.

3.3.2. Stator exit/Rotor inlet measurements Plane 2

Measurements between the stator vanes and rotor blades are primarily used to characterize the flow at the inlet of the rotor and be used as validation for the results of CFD studies in this region. The flow in this region is characterized by high Vane exit mach numbers that, with the reduced space available between Vane TE and Blade LE, makes the measurement in this region risky for the probe mechanical integrity and on the quality of the flow measurements, therefore the axial location of this plane will be set based on safety clearance assessed by structural analysis and numerical CFD investigations.The measurements will be taken traversing a multi-head Kiel probe and a single-head five-hole probe to determine total pressures and flow angles respectively. Continuous traverses will be performed by an actuated mechanism in the pitchwise direction during each blowdown. A refined measurement matrix is also achieved traversing the probe in the radial direction. In addition to the traverses, measurements of time-averaged and time-resolved static pressure will be taken on the hub and shroud endwalls at the same axial location as plane 2.

3.3.3. Stage exit measurements Plane 3

To fully characterize the flow downstream of the blade, measurements at the exit of the stage are to be taken by a numerous type of instrumentation. This region is characterized by unsteady, three-dimensional flow where the complex interactions between the hub and shroud leakage flows and the mainstream flow are not very well understood, posing challenges to the aerodynamic design of the hardware (blades, cavities, endwalls) and resulting in inefficiencies in the engine. The flow-field in this region will be characterized in terms of total pressure, flow-angle and total temperature. All of the above measurements will be made by traversing the probes in both the radial and circumferential directions along plane 3. Further to the measurements in the mainstream flow-path, a large number of measurements will also be taken at stationary endwalls downstream of the blades using pressure taps and unsteady static pressure sensors on the hub and tip endwalls. Higher number of fast-response pressure sensors is envisaged on the hub endwall to capture the higher instability expected at the hub and to relate the higher number of variances given by the test matrix, described later.

3.3.4. Hub upstream and downstream cavity measurements

Measurements in the upstream and downstream hub cavities are used to characterize the flow structure within the cavities and to determine the boundary conditions at the cavity-mainstream interface. Time-averaged and time-resolved static pressure measurements, total pressure and gas temperature at various

Table 3: Experimental campaign test matrix

Operating Conditions	**Configurations**	
	Nominal Tip Clearance	***High Tip Clearance***
Nominal Speed Nominal Purge Nominal Swirl	Test Case 1 Reference Case (All Measurements)	Test Case 2 (Plane 3 Measurements Only)
Nominal Speed Nominal Purge Low Swirl	Test Case 3 (Plane 3 Measurements Only)	-
Nominal Speed High Purge Nominal Swirl	Test Case 4 (Plane 3 Measurements Only)	-
High Speed Nominal Purge Nominal Swirl	Test Case 5 (All Measurements, No Plane 1)	Test Case 6 (Plane 3 Measurements Only)

radial and circumferential locations within the cavities are envisaged. Unsteady static pressure at the civity rim seals will be measured using eight Kulite transducers placed at eight different circumferential location around the wheels-space in order to enable a phase analysis of the unsteady signal and hence the determination of the number of unsteady flow structures that are known to form in these regions. Temperature measurements will be used to investigate the ingress/egress between the mainstream flow path and the cavity and the effectiveness of the rim-seals. Measurements of time-averaged static pressure and temperature will also be taken further inboard (Fig. 3), inside the wheel-space, at various radial locations. The total pressure will be measured using small pitot-tubes positioned at the same radial location as the pressure taps, at 5 mm off the surface of the stator walls. The pair of static and total temperature at each radial location will be used to determine the tangential velocity of the flow and hence the swirl ratio which in turn provides an indication of the flow structure inside the wheel-space. To determine the amount of purge flow leaking through the labyrinth seals and out of the cavities, measurements of static pressure will be taken on either side of the tooth of the upstream and downstream labyrinth seals.

3.3.5. Shroud cavity measurements

Measurements in the shroud cavity are used for characterizing the flow-field within this cavity and for determining the performance of the blade tip seals. Measurements of time-averaged static pressure will be taken at various axial and radial locations along the cavity using, as shown in Fig. 3. Measurements of time-resolved static pressure will be taken using Kulite sensors positioned in the three cavities formed between the lips of the blade tip-seal. At each of these locations two sensors will be used, placed at two different circumferential locations aligning with the vane leading edge and mid-pitch.

3.4. Test Matrix

The measurements mentioned in the preceding sections are to be taken for a number of combinations of operating conditions and geometric variations (referred to as configurations) involving two operating speeds, two purge flow rates and injection angles and two shroud cavity clearance variations. The resulting test matrix is given in Table 3.

Test case 1 represents the reference case. Comparison of the results of test case 1 and test case 2 aims at revealing the effect of the tip clearance variation on the flow-field downstream of the blades, near the tip region, and the subsequent effect on the efficiency of the rotor. Comparison of the results of test cases 1 and 3 aims at shedding light into the effect of hub purge flow swirl on the flow-field upstream of the blades, near the hub region, and on the subsequent effect on the efficiency of the rotor. Comparison of the results of test cases 1 and 4 aims at revealing the effect of hub purge flow increase on the flow-field upstream of the blades, near the hub region, and the on the subsequent effect on the efficiency of the rotor. Comparison of the results of test cases 1 and 5 will reveal the effect of under-speed operating conditions on the flow-field and efficiency or the rotor and lastly, comparison between test cases 5 and 6 will shed light into the effect of tip-clearance variation during under-speed operation of the turbine.

4. Prelinimary Design Of The SPLEEN 1-Stage LPT

To accommodate the flow-path geometry of the SPLEEN 1-stage LPT turbine, it was necessary a redefinition of the available-space region, based on facility hard constraints. The high aspect ratio of the

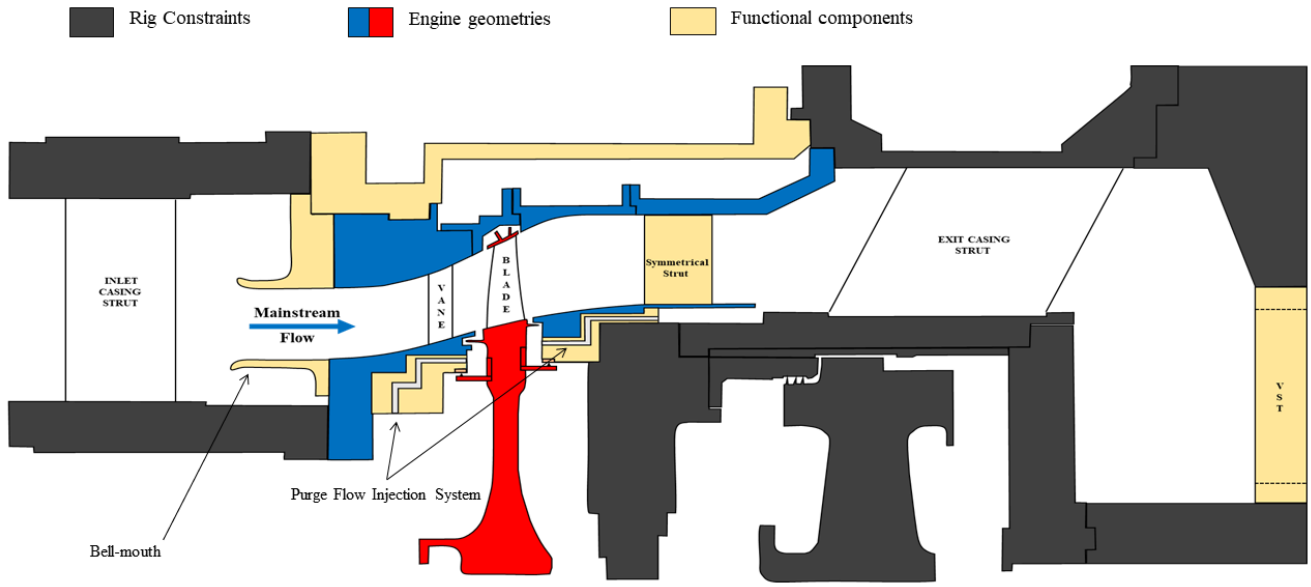

Figure 4: Overview of the preliminary facility redesign

new low pressure module, imposed a redesign of the rotating assembly (disk, lab seals and blades) as well as an extension of the radial geometrical envelop to include the new gaspath. The initial design phase of gaspath and stage was performed through an extensive coordination with the industrial partner Safran Aero Engines to embed the engine geometries within the hard constraint of the facility. An extensive revamping of the fixed facility modules is requested to ensure testing. Figure 4 shows the different modules of the facility underlining in grey the facility hard constraints. In blue and red are reported respectively the static and rotating engine geometries designed by SAE. In yellow the functional and auxiliary components designed by the research team of the Von Karman Isntitute. The latter are:

- Intake bell-mouth designed by means of numerical tools to ensure the smallest boundary layer thickness and to avoid risk of flow separation at the lip leading edge, given the available space envelope;
- Purge flow injection designed by means of 3D annular parametric CFD study intended to select the optimal swirling injecting angle and discrete injection parameters to ensures the target mass flow and velocity ratios (V_t/U) at the two hub cavities.
- The symmetrical exit struts embedded in the gas path, which geometrical characteristics are chosen to ensure the lowest intrusiveness in the upstream stage aerodynamics, serve the purpose to provide access for purge supply lines for the downstream wheel-space and instrumentation lead-out.
- Variable Sonic Throat (VST) - used to regulate the mass flow rate of the mainstream flow passing through the turbine. The maximum available cross-sectional area of the VST currently installed in CT-3 is not sufficient to ensure the high capacity requirements of the SPLEEN 1-stage LPT. A new VST is to be designed featuring openings with a larger area. The design of the new VST is to be aided by a CFD study that aims at validating the new area requirements.

4.1. Bellmouth

The intake assembly consists of the inner and outer intake lips and is used for setting the conditions of the flow at the inlet to the turbine, upstream of vane 1. The section of the intake lips is specifically designed so that the lips together form a bell-mouth inlet that accelerates the flow, keeping the boundary layer thickness within the required value and avoiding flow separation and distortion at the leading edge. A literature survey showed that the best design for the inlet bell-mouth is provided when an elliptical shape

is selected. Tawari et Al. [16] use numerical simulations to compare different intake design: 3-circle profiles, airfoil profiles and elliptical shapes. Both 3-circle and airfoil profiles require steeper inlet contraction to fulfill small inlet boundary layer thickness and to avoid separation, leading to increase the diameter at the entry. Blair and Cahoon [17] report an extensive experimental and numerical investigation of bell-mouth intakes with circular, airfoil-shaped and elliptical profiles, comparing the discharge coefficient of each design. Bell mouth with elliptical shapes show the highest discharge coefficient with the optimum results of ellipses with major-over-minor axis aspect-ratio = 1.8. A modified super elliptical (MSE) splitter plate ensures second derivative continuity on the transition from elliptical to planar shapes, therefore low susceptivity of the boundary layer from freestream flow perturbations ([18], [19], [20]). Planar 2D numerical RANS have been performed to validate the intake bellmouth design of the SPLEEN experimental apparatus, using the commercial software Numeca FINE/Open. Curvature continuity is ensured over the intake bell-mouth elliptical shape and at the junction with the gas path. A total of four different design have been investigated, differing from the elliptical lip aspect-ratio. The bottom lip is constrained by space, therefore a compact design shall be selected. Figure 5 shows an example of numerical 2D domain and the different geometries tested. ‘

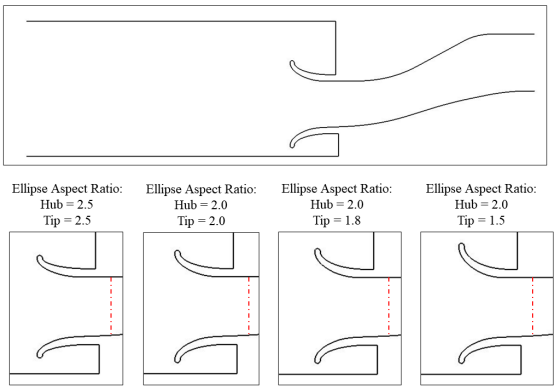

Figure 5: Intake bell-mouth numerical 2D domain (Top) and studied shapes (Bottom). Dash-dot red line indicates the evaluation plane

Fully turbulent numerical simulation have been performed using $k-\omega$ SST turbulence model. Stage Total inlet pressure and temperature, and outlet mass flow were imposed. The selected inlet turbulence intensity of 6% as measured from previous campaigns

Table 4: Boundary layer thickness at measurement plane

	δ_{99} **[mm]**	
Geometry	**Hub**	**Tip**
Symm AR =2.5	3.56	2.78
Symm AR =2.0	2.91	2.78
H AR = 2 — T AR = 1.8	2.91	2.14
H AR = 2 — T AR = 1.5	2.91	2.14

performed in CT-3. The investigation plane is located at the junction between gaspath and bell-mouth lips, indicated by the dash-dot red line in Figure 5. This plane was selected because provides the inlet of the test section. Table 4 reports the boundary layer thickness and shows that higher contraction ensures smaller boundary layer thickness. The selected design the design with symmetric lips at the top and at the bottom with aspect ratio. In this case a similar boundary layer thickness is measured both at the hub and tip lips, still displaying values below 3mm.

4.2. Symmetrical Struts

The main purpose of the symmetrical struts is to allow for access for purge lines and instrumentation cable/tube lead-out. The outlet flow delivered from the test section is swirling compressible flow (α = 30deg. , M = 0.38). The accurate design of the symmetrical strut is performed to reduce the potential flow effects on the upstream stage and instrumentation yet maintaining a simple design for manufacturing purposes. The selected airfoil shape is the NACA0024 selected to guarantee highest thickness and therefore the highest available space for piping and cabling. The airfoils axial chord is equal to 70 mm, maximum length constrained by the available space. A parametric analysis was undertaken to investigate the effect of 12, 18 or 24 struts located around the annulus. The evaluation of the design is performed by means of 2D numerical simulations with translational periodicity in accordance with the struts periodicity. The inlet boundary conditions are summarized in Table 5. Fully turbulent simulations have been performed using the $k-\omega$ turbulence model. The outlet static pressure imposed was selected iteratively to match the flow rate.

Figure 6 shows the static pressure contours of the test case with 24 struts around the annulus. In Figure 7 is reported the static pressure fluctuations along the pitch for the cases with 18 and 24 struts at different axial locations from the upstream Blade TE. An admissible fluctuation of static pressure below 0.1% $P_{0,in}$ (100 Pa) is targeted. 12 struts generate a fluctua-

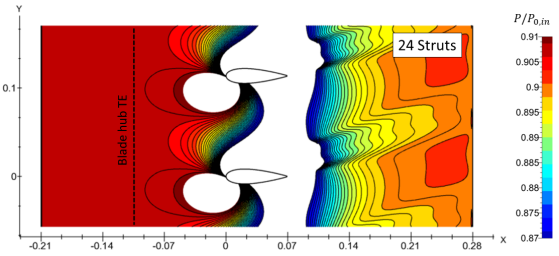

Figure 6: Static pressure contours prediction around the symmetrical strut. Case with 24 struts around the annulus

Table 5: Inlet boundary conditions of CFD simulations on the symmetrical struts aerodynamics

Quantity	**Value**
$P_{0,in}$ [Pa]	38926.97
$T_{0,in}$ [K]	271.6
Inlet Angle [$\circ$]	30.0
Tu [%]	2.5

tion over 0.1% at the blade TE, representing an unacceptable value and therefore not reported here. Considering the cavity opening and the space required for instrumentation, static pressure variation shall be kept within uncertainty up to at least 1 axial chord downstream the blade TE. This condition is respected when 18 or 24 struts are employed, although with noticeable improvement for 24 struts. In this case the available space can be extended over 1.5 axial chords and therefore represents the safest design. Furthermore, the total pressure losses ($(P_{0,in}$-$P_0)/P_{0,in}$) accounted for this design is of 1.14%, which represent an acceptable increment with respect to he case with 18 struts, accounting for a total pressure loss of 0.93%.

4.3. Variable Sonic Throat

The operative condition of the Variable Sonic Throat (VST) is examined by means of 3D RANS simulations. The study is performed to quantify the admissible mass flow rates flowing through the choked throat to identify the limitations of the facility. Two designs of the VST are investigated:

- Component currently installed in CT3 with maximal admissible cross sectional opening
- New VST design for testing turbines at higher capacities, increasing the cross-sectional opening of 35%.

These two designs have been tested with the inlet swirl angle and inlet total pressure measured downstream of the symmetric exit struts from the analysis described in the previous section. The analysis was run for testing condition with nominal Turbine Reynolds number with a target mass flow through the turbine of 10.57 [kg/s]. Table 6 reports inlet and outlet boundary conditions. The fluid domain includes the exit casing strut (Figure 4) and the variable sonic throat. The turbulence model $k-\omega$ was selected for the fully turbulent simulations. The maximum mass flow rate and discharge coefficient for the two VST designs are reported in Table 7. Both designs ensure the operating condition of the SPLEEN LPT, although the current design show a limited safety margin ($< 25\%$) therefore the design with increased cross-sectional area was selected.

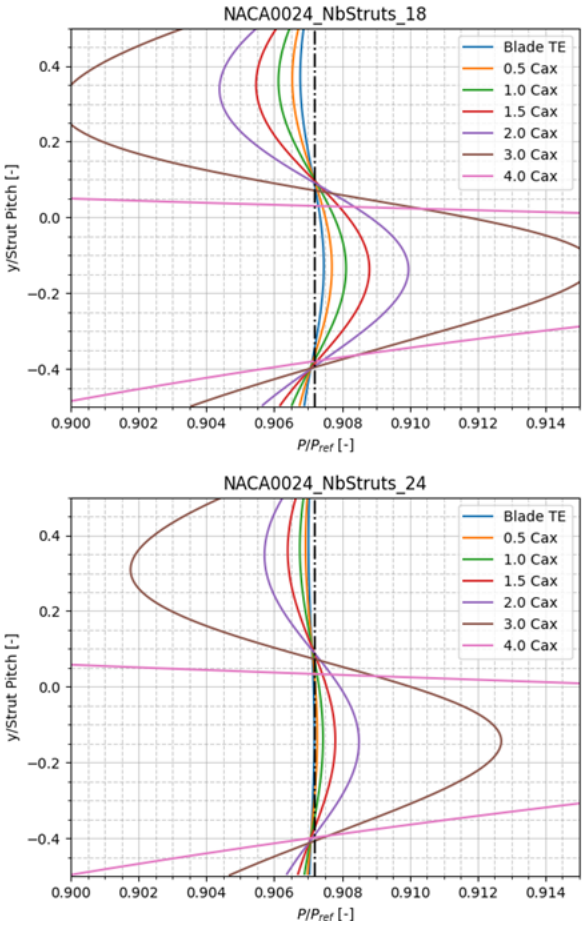

Figure 7: Pitch-wise static pressure variation at different axial position for the blade TE location. Static pressure normalized by the inlet total pressure. Case with 18 (Top) and 24 (Bottom) struts around the annulus

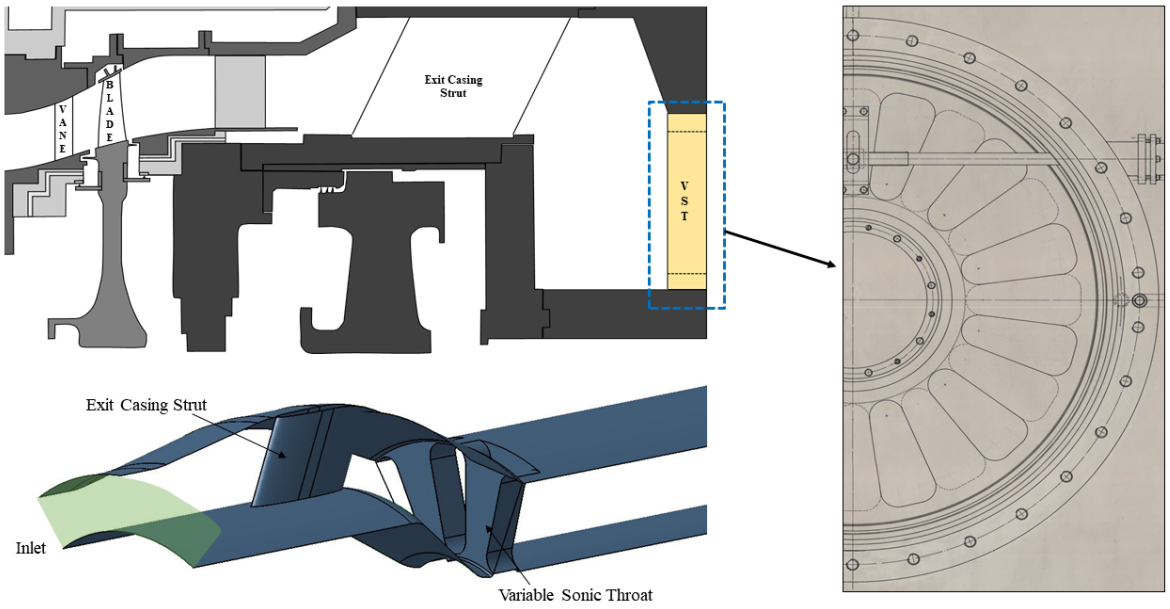

Figure 8: Variable sonic throat sketched in the rig (Top-Left). Current VST Design (Right) and CFD domain (Bottom-Left)

Table 6: VST numerical study - Boundary conditions

Quantity	**Value**
$P_{0,in}$ [Pa]	38460.32
$T_{0,in}$ [K]	271.56
Inlet Angle [$\circ$]	17.86
Pout [Pa]	15000
P0_in/Pout [-]	2.6

Table 7: VST Design Results

VST Size	$\dot{m}$ **[Kg/s]**	C_D [-]
Current Design	12.63	0.839
Enlarged Area +35%	16.78	0.832

5. Conclusion

This paper introduced the experimental apparatus of the Von Karman Institute to operate and test the new High-Speed Low Pressure Turbine module. The detailed test matrix will allow a decomposition of the different elements playing a role in the turbine efficiency and to retrieve the effect of each features. Meaningful data and useful information on the effect of cavity flows and purge variation in High-Speed LPT representative environment. The turbine efficiency will be measured, also evaluating the impact of the off-design velocity triangles on turbine losses and output work. As discussed, the facility will be heavily instrumented to capture the 3D flowfield both upstream and downstream of the rotor blade. Fast response pressure sensors will be used to measure the unsteady features rising in the turbine at the hub cavities location and on the shroud casing. Fast Response miniaturized probe will measure the unsteady flow angles at the rotor exit. In the paper is also presented the preliminary design selection for the revamping of the Von Karman Institute compression tube facility CT-3, to house the new High-Speed Low Pressure Turbine module. The redesign of the intake bell-mouth is discussed and the simulation performed predict boudary layer thickness about 10% of the blade axial chord. The new design of the variable sonic throat is discussed. It allows a safe operating conditions of the LPT module with a safety margin over 50% of the targeted mass flow rate. The auxiliary structural elements located dowsntream of the stage are also analysed. Their number around the annulus was optimised to reduce the potential effect upstream,and to limit the impact on the instrumentation. The numerical results show low effect on the static pressure fluctuation below 0.1% of the total inlet pressure on the measurement region located dowstream of the rotor TE.

Acknowledgments

The authors gratefully acknowledge funding of the SPLEEN project by the Clean Sky 2 Joint Undertaking under the European Unions Horizon 2020 research and innovation programme under the grant agreement 820883.

References

[1] Internation Civil Aviation Organization, Table of the traffic forecast, https://www.icao.int/sustainability/Documents/tables\%20of\%20the\%20traffic\%20forecasts_v2.pdf, (2018).

[2] EU, Flightpath 2050 europes vision for aviation, https://ec.europa.eu/transport/sites/transport/files/modes/air/doc/flightpath2050.pdf, (2011).

[3] J. Kurzke, Fundamental differences between conventional and geared turbofans, volume 1: Aircraft Engine; Ceramics; Coal, Biomass and Alternative Fuels; Controls, Diagnostics and Instrumentation; Education; Electric Power; Awards and Honors (Jun 2009). doi:10.1115/GT2009-59745.
URL https://doi.org/10.1115/GT2009-59745

[4] D. Torre, Design and testing of a multi-stage ip turbine for future geared turbofans, 2020.

[5] M. Giovannini, F. Rubechini, M. Marconcini, A. Arnone, F. Bertini, Analysis of a lpt rotor blade for a geared engine: Part i - aero-mechanical design and validation, 2016. doi:10.1115/GT2016-57746.

[6] F. Malzacher, J. Gier, F. Lippl, Aerodesign and testing of an aero-mechanically highly loaded lp turbine, Journal of Turbomachinery-transactions of The Asme - J TURBOMACH-T ASME 128. doi:10.1115/1.2172646.

[7] A. Mahallati, B. Mcauliffe, S. Sjolander, T. Praisner, Aerodynamics of a low-pressure turbine airfoil at low reynolds numbers-part i: Steady flow measurements, Journal of Turbomachinery 135 (2013) 011010–011010. doi:10.1115/1.4006319.

[8] A. Mahallati, S. Sjolander, Aerodynamics of a low-pressure turbine airfoil at low reynolds numbers-part ii: Blade-wake interaction, Journal of Turbomachinery 135 (2013) 011011–011011. doi:10.1115/1.4006320.

[9] M. Börner, R. Niehuis, Dynamics of shock waves interacting with laminar separated transonic turbine flow investigated by high-speed schlieren and surface hot-film sensors, volume 2B: Turbomachinery (Sep 2020). doi:10.1115/GT2020-14386.
URL https://doi.org/10.1115/GT2020-14386

[10] M. Giovannini, F. Rubechini, M. Marconcini, D. Simoni, Y. Vianney, F. Bertini, Secondary flows in lpt cascades: Numerical and experimental investigation of the impact of the inner part of the boundary layer, 2018. doi:10.1115/GT2018-76737.

[11] H.-P. Wang, S. J. Olson, R. J. Goldstein, E. R. G. Eckert, Flow visualization in a linear turbine cascade of high performance turbine blades, 1995. doi:10.1115/95-GT-007.

[12] M. Vera-Morales, E. Blanco, H. Hodson, R. Vazquez, Endwall boundary layer development in an engine representative four-stage low pressure turbine rig, Journal of Turbomachinery-transactions of The Asme - J TURBOMACH-T ASME 131. doi:10.1115/1.2952382.

[13] M. Lipfert, J. Habermann, M. Rose, S. Staudacher, Y. Guendogdu, Blade-row interactions in a low pressure turbine at design and strong off-design operation, Journal of Turbomachinery 136 (2014) 111002. doi:10.1115/1.4028213.

[14] P. Jenny, R. Abhari, M. Rose, M. Brettschneider, J. Gier, A low pressure turbine with profiled end walls and purge flow operating with a pressure side bubble, Journal of Turbomachinery 134.

[15] C. H. Sieverding, T. Arts, The vki compression tube annular cascade facility ct3, volume 5: Manufacturing Materials and Metallurgy; Ceramics; Structures and Dynamics; Controls, Diagnostics and Instrumentation; Education (Jun 1992). doi:10.1115/92-GT-336.
URL https://doi.org/10.1115/92-GT-336

[16] A. Tiwari, S. Patel, A. Lad, C. Mistry, Development of bell mouth for low speed axial flow compressor testing facility, 2016.

[17] Blair, G. P. and Cahoon, W. M., Design of an intake bellmouth, http://www.profblairandassociates.com/pdfs/RET_Bellmouth_Sept.pdf,.

[18] N. Lin, H. L. Reed, W. S. Saric, Effect of leading-edge geometry on boundary-layer receptivity to freestream sound, in: M. Y. Hussaini, A. Kumar, C. L. Streett (Eds.), Instability, Transition, and Turbulence, Springer New York, New York, NY, 1992, pp. 421–440.

[19] R. E. Hanson, H. P. Buckley, P. Lavoie, Aerodynamic optimization of the flat-plate leading edge for experimental studies of laminar and transitional boundary layers, 2012.

[20] C. Tropea, A. Yarin, J. Foss, Springer Handbook of Experimental Fluid Mechanics, 2007. doi:10.1007/978-3-540-30299-5.